

REVERSE TIME MIGRATION IN TILTED TRANSVERSELY ISOTROPIC MEDIA

Razec Cezar Sampaio Pinto da Silva Torres and Leandro Di Bartolo

ABSTRACT. Reverse time migration (RTM) is one of the most powerful methods used to generate images of the subsurface. The RTM was proposed in the early 1980s, but only recently it has been routinely used in exploratory projects involving complex geology – Brazilian pre-salt, for example. Because the method uses the two-way wave equation, RTM is able to correctly image any kind of geological environment (simple or complex), including those with anisotropy. On the other hand, RTM is computationally expensive and requires the use of computer clusters. This paper proposes to investigate the influence of anisotropy on seismic imaging through the application of RTM for tilted transversely isotropic (TTI) media in pre-stack synthetic data. This work presents in detail how to implement RTM for TTI media, addressing the main issues and specific details, e.g., the computational resources required. A couple of simple models results are presented, including the application to a BP TTI 2007 benchmark model.

Keywords: finite differences, wave numerical modeling, seismic anisotropy.

RESUMO. A migração reversa no tempo (RTM) é um dos mais poderosos métodos utilizados para gerar imagens da subsuperfície. A RTM foi proposta no início da década de 80, mas apenas recentemente tem sido rotineiramente utilizada em projetos exploratórios envolvendo geologia complexa, em especial no pré-sal brasileiro. Por ser um método que utiliza a equação completa da onda, qualquer configuração do meio geológico pode ser corretamente tratada, em especial na presença de anisotropia. Por outro lado, a RTM é dispendiosa computacionalmente e requer o uso de *clusters* de computadores por parte da indústria. Este artigo apresenta em detalhes uma implementação da RTM para meios transversalmente isotrópicos inclinados (TTI), abordando as principais dificuldades na sua implementação, além dos recursos computacionais exigidos. O algoritmo desenvolvido é aplicado a casos simples e a um *benchmark* padrão, conhecido como BP TTI 2007.

Palavras-chave: diferenças finitas, modelagem numérica de ondas, anisotropia sísmica.

INTRODUCTION

Proposed by Baysal et al. (1983) almost 40 years, reverse time migration (RTM) is a method that currently attracts great attention from academy and oil & gas industry. The RTM has no restrictions regarding dip of the geological layers and lateral variations in the propagation velocity of the media. The method is able to produce excellent subsurface images, even in very complex geology contexts. The major drawback of RTM is the high computational demand.

RTM algorithm solve two times the wave equation by some numerical method. First, the wavefield is propagated, from the source to the interior of the layers in forward time and the receiver wavefield is propagated in reverse time, from receivers to the interior of the model. Through the two fields propagated, for example using the finite difference method, one can apply an image condition to construct the subsurface image. The most conventional image condition used currently in pre-stack RTM is the cross correlation. The seismic data is, in general, migrated one by one, so, the generated images of each shot are stacked at the end.

As it uses the complete wave equation, RTM is capable to generate images with superior quality compared to Kirchhoff migration, especially in challenging environments. The reason is it correctly handles the different wave paths and the chaotic wave propagation due to complexity of geological formations. Therefore, it has been successfully applied to anisotropic media, especially in transversely isotropic (TI) media. However, RTM

algorithms that consider the anisotropy are more computationally expensive because there is a great number of parameters involved. Hence, RTM in TI media presents itself as a challenge application in industry, considering the large amounts of data, especially in 3D acquisitions.

As has been known for more than a century (Rudzki, 1897), the elastic properties of rocks in geological formations vary with the direction of seismic wave propagation.

Rudzki (1912) discusses the propagation of elastic waves in TI media. Nevertheless, only in the last 40 years has anisotropy had a significant impact in the area of hydrocarbon exploration, mainly due to computational evolution, which allowed the use of more refined models and algorithms than the isotropic approaches (Helbig & Thomsen, 2005). In recent years this impact has grown considerably.

Rudzki predicted that a diversity of rocks could be anisotropic in nature, which was proven experimentally only years later. Today it is known that several classes of anisotropy are found in nature, namely, monoclinic, orthotropic (or orthorhombic), tetragonal, trigonal, cubic and TI (Bos et al., 2004). Therefore, it is extremely important to consider the existence of anisotropy, as thus the wavefields are correctly represented and, ultimately, for the correct positioning of the reflectors. On the other hand, the large offsets of current acquisitions, typically around 10 km, have substantially increased the impact of anisotropy on current seismic data. Thus, algorithms that do not consider anisotropy end up generating low quality results.

The isotropic pre-stack RTM algorithms are not sufficient to produce satisfactory results. The consideration of transversely isotropic models (TI) is quite satisfactory for a large number of rock formations, with the advantage of presenting a reduced number of parameters. Vertical transverse isotropy (VTI) is a class of anisotropy where axis of symmetry is vertical. VTI media are characterized by the invariance of the elastic properties under rotation about the vertical z-axis. In tilted transverse isotropic (TTI) media, the symmetry axis is tilted. In the TTI case, the modeling presents 7 elastic parameters - we can think in terms of the P and S wave velocity, more three Thomsen anisotropy parameters (Thomsen, 1986) and two dip angles of the symmetry axis. In this sense, in furthermore to the problem of high computational cost, the application of RTM TTI algorithms presents itself as extremely challenging.

A very common approach in the literature to reduce the cost problem is the use of pseudo-acoustic (PA) equations instead of the general elastic equations for TTI media. The PA equations are second order coupled equations in which the objective is to model only the P wavefield. Alkhalifah (2000) proposed the first PA equation for VTI media and other authors proposed different equations for VTI media moreover the extensions of these equations for the TTI case (Zhou et al., 2006; Fletcher et al., 2009; Fowler et al., 2010). The use of these equations in reverse time migration over time is extremely advantageous

from a computational point of view, as it substantially improves computational efficiency and allows to reduce the number of elastic parameters involved.

Considering TTI media, in areas where there is a strong variation of the anisotropic parameters, especially the angle of inclination of the symmetry axis (as in anticlines formed in halokinesis environment), it can result in instabilities in the direct and "reverse" modeling used in the RTM. One way to make it more stable is to use a PA formulation that considers the S wave velocity to be non-zero (Fletcher et al., 2009). In these equations, the degree of instability is controlled by a parameter that can be manipulated, being responsible for the propagation of the S wave (for P wave implementation is considered an artifact in RTM).

This work proposes to investigate the influence of anisotropy on seismic imaging through the application of RTM for TTI media in pre-stack data. The results were obtained for the acoustic isotropic case and for the TTI case, in order to qualitatively compare the main characteristics that differ the two approaches. Details of the implementation of the RTM for TTI media are presented, addressing the main difficulties in its implementation, in addition to the required computational resources. Altogether, three case studies were applied on synthetic data, the degree of complexity of the media increasing for each case and the last case being applied to a BP TTI 2007 benchmark.

METHODOLOGY

The first part of an RTM algorithm corresponds to direct modeling of seismic wave propagation, e.g., the data is modeled from the source to the deep rock layers. Thus, it models the effects of the wave propagation using a mathematical equation that describes the physical behavior of the wave. In this work, pseudo-acoustic (PA) equations proposed by Fletcher et al. (2009) for TTI media were used. Subsequently, a reverse time modeling is made together the application of image condition.

Forward Problem

The TTI media has a tilt angle θ on the axis of symmetry, different from VTI media in which the axis of symmetry is vertical (Fig. 1).

The TTI pseudo-acoustics is obtained through the P-SV dispersion relation for TTI media, given by:

$$\begin{aligned} \omega^4 = & [(v_{px}^2 + v_{sz}^2)\hat{k}_x^2 + (v_{pz}^2 + v_{sz}^2)\hat{k}_z^2]\omega^2 \\ & - v_{px}^2 v_{sz}^2 \hat{k}_x^4 - v_{pz}^2 v_{sz}^2 \hat{k}_z^4 \\ & + [v_{pz}^2(v_{pn}^2 - v_{px}^2) \\ & - v_{sz}^2(v_{pn}^2 + v_{pz}^2)] \times \hat{k}_x^2 \hat{k}_z^2 \end{aligned} \quad (1)$$

where, \hat{k}_x, \hat{k}_y and \hat{k}_z are the components of wave number vector in a rotated coordinate system, ω is the angular frequency, v_{pz} is the P wave velocity in the parallel direction to the axis of symmetry, $v_{pn} = v_{pz}\sqrt{1 + 2\delta}$ is the P

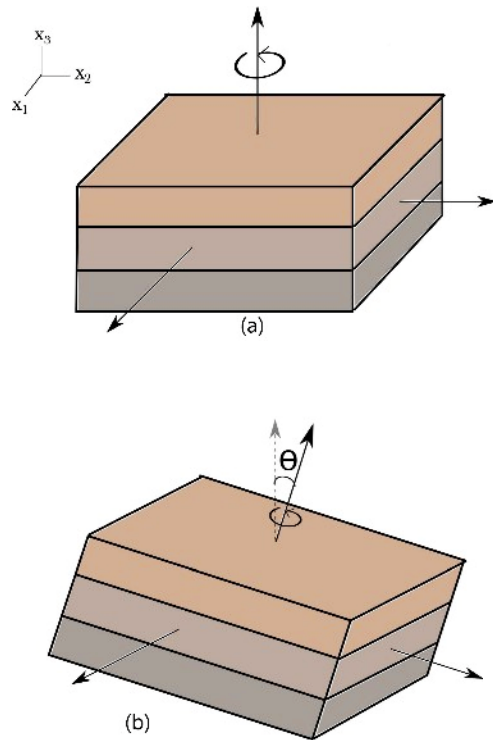


Figure 1 – (a) vertical transversely isotropic (VTI) media and (b) tilted transversely isotropic (TTI) media.

normal moveout velocity, $v_{px} = v_{pz}\sqrt{1 + 2\epsilon}$ is the P wave velocity in horizontal direction, v_{sz} is the SV wave velocity, and δ and ϵ are the anisotropic parameters proposed by Thomsen (1986). According to Fletcher et al. (2009) the TTI PA equations are (2D):

$$\begin{aligned} \frac{\partial^2 p}{\partial t^2} = & v_{px}^2 H_2 p + \alpha v_{pz}^2 H_1 q + \\ & v_{sz}^2 H_1 (p - \alpha q), \\ \frac{\partial^2 q}{\partial t^2} = & \frac{v_{pn}^2}{\alpha} H_2 p + v_{pz}^2 H_1 q \\ & - v_{sz}^2 H_2 \left(\frac{1}{\alpha} p - q \right) \end{aligned} \quad (2)$$

where the differential operators H_1 and H_2 are being θ the angle in relation to the z-axis:

$$H_1 = \sin^2\theta \frac{\partial^2}{\partial x^2} + \cos^2\theta \frac{\partial^2}{\partial z^2} + \sin 2\theta \frac{\partial^2}{\partial x \partial z}, \quad (3)$$

$$H_2 = \frac{\partial^2}{\partial x^2} + \frac{\partial^2}{\partial z^2} - H_1$$

The Equation (2) consider a finite value of qS wave velocity in modeling. This component is important because it can reduce problems with instabilities on modeling, especially in environments where there is a strong variation of the angle in relation to the axis of symmetry. The amount of qS wave in the modeling is controlled through the sigma parameter, which is given by:

$$\sigma = \frac{v_{pz}^2}{v_{sz}^2} (\varepsilon - \delta). \quad (4)$$

In Figure 2, we can see two cases of qP and qS waves snapshots for VTI and TTI homogeneous media. In the first case, the qS velocity is zero, Figures 2a and 2c. The second case, Figures 2b and 2d, set a value for qS velocity, estimated through the Equation (4) using $\sigma = 0.7$.

Finite difference modeling

For the solution of the acoustic and pseudo-acoustic equation TTI (Eq. 2), the method of finite differences was applied. An algorithm of explicit time marching was used with second order approximations in time. For spatial approximation, fourth order was applied to the acoustic isotropic case and eighth order was applied to the TTI PA case.

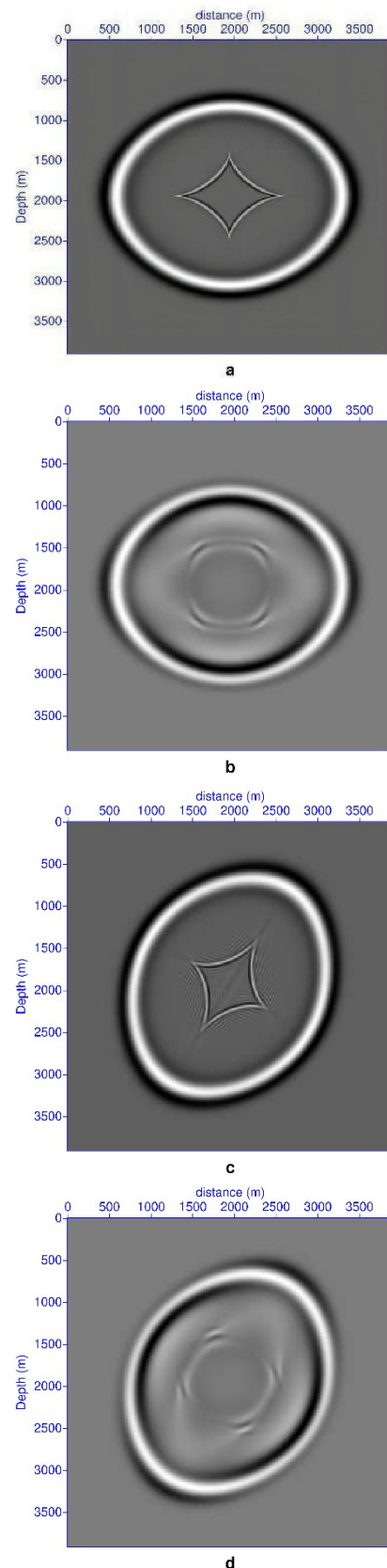


Figure 2 – Snapshots for (a) and (b) VTI and (c) and (d) TTI media ($t = 0.4$ s). The parameters used were $v_{pz} = 3000$ m/s, $\varepsilon = 0.24$, $\delta = 0.1$, and $\theta = 60^\circ$.

Non-dispersion condition and stability

The grid spacing (h), which is equal in both x and z directions ($h = \Delta x = \Delta z$), was calculated by the relation:

$$h \leq \frac{v_{min}}{\alpha f_{cut}}, \quad (5)$$

as well as the time step by:

$$\Delta t \leq \frac{h}{\beta v_{max}}, \quad (6)$$

where v_{min} is the minimum velocity of the model, v_{max} is the maximum velocity of the model, f_{cut} is the maximum frequency of the seismic source, and α, β are constants. Such criteria are of high importance in seismic modeling to avoid dispersion and ensure the stability and the accuracy in numerical solution. It is recommended to use at least $\alpha = 5$ and $\beta = 4$, for second order approximation in time and fourth order approximation in space.

Reverse Time Migration

In reverse modeling, the seismic waves that were recorded at the receivers during seismic acquisition are propagated in the opposite direction of time. This procedure is performed by injecting the energy from the seismogram to the model, towards the reflectors in the subsurface. It is in the reverse modeling stage that the image condition is applied.

Modeling the propagation of wavefields in the reverse direction of time is valid due to the principle of temporal reversibility. It states that solving the wave equation in the reverse direction of time preserves the physical and mathematical properties, that is, the wavefield is symmetric in relation to time (Zhu, 2014). Another important foundation is the reciprocity theorem. It states that, under certain conditions, developing a seismic experiment for a receiver-source arrangement in a given position and then change this position between source and receiver to the same previous position, does not alter the wavefield (Ramírez & Weglein, 2009). Therefore, these two principles support the RTM.

Image condition

The image condition is responsible for generating the seismic image in depth. There are many image conditions, but in this work we choose the conventional zero-lag cross correlation, based on the imaging principle proposed by Claerbout (1971). Once all wavefields propagated in the forward and reverse direction in time are obtained, a seismic reflector is identified in space and time through the zero-lag cross correlation between these two wavefields. The propensity is that in the reflector, there is a constructive interference in the wave's amplitudes and in the other positions yields in a destructive interference, consequently an image of the subsurface is obtained. The following relation gives the 2D image condition by cross correlation:

$$I(x, z) = \int_{t=0}^{\infty} \frac{S(x, z, t).R(x, z, t)}{|S(x, z, t).S(x, z, t)|} dt, \quad (7)$$

where t is the modeling time, $S(x, z, t)$ is the source wavefield, $R(x, z, t)$ is the receivers wavefield and $I(x, z)$ is the image.

In Equation (5), we can notice that the image was divided by the autocorrelation of the source field. This action is able to generate an amplitude compensation for the image. It is due to the loss of energy in the wave propagation generate by spherical divergence.

RESULTS AND DISCUSSION

In this work, three different models were subject to the TTI pre-stack RTM algorithm implemented, generating three different case studies. In each model there is an increase in complexity. The last one was the BP TTI 2007 benchmark model, a realistic model with a salt dome structure.

Case study I

The first case study was developed for the anisotropic TTI model, shown in Figure 3. Although it is relatively simple, it is useful to validate the RTM TTI algorithm. The P wave velocity model in vertical direction and anisotropic parameters are shown together (Fig. 3).

The inclined model simulates an anisotropic environment with inclinations in opposite directions and which does not necessarily have a realistic geological correlation. This model has a length of 1,800 km on the z-axis and 3,600 km on the x-axis. Regarding the P wave velocity model, the first layer represents the water depth with a value equal to 1500 m/s, the background velocity is equal to 2000 m/s and in the inclined layer, it has a value of 2500 m/s. The anisotropy is concentrated in the steepest layer, where the values of ε and δ are equal to 0.24, 0.1, respectively. The only part of the model that is anisotropic is the layer with the inclinations, in which it has angles equals to $+45^\circ$ and -45° and everything else the anisotropic parameters are zero (Fig. 3).

The seismic data was generated using Equation (2). The grid space used was $h = 12$ m and a Ricker wavelet of 30 Hz cutoff frequency was applied. The geometry of data acquisition was of fixed spread of receivers and with the seismic source moving with a spacing of 36 m, with a total of 100 shots. The results for acoustic isotropic RTM and TTI pseudo-acoustic RTM are shown at Figure 4.

The results for acoustic isotropic RTM and TTI are very similar, although a slightly improved signal-to-noise image is obtained for TTI case (see e.g. the noise pointed by the arrow in Fig. 4a). The similarity is due to the small horizontal distance between source and receivers, making the wave to propagate in a direction near from the vertical one.

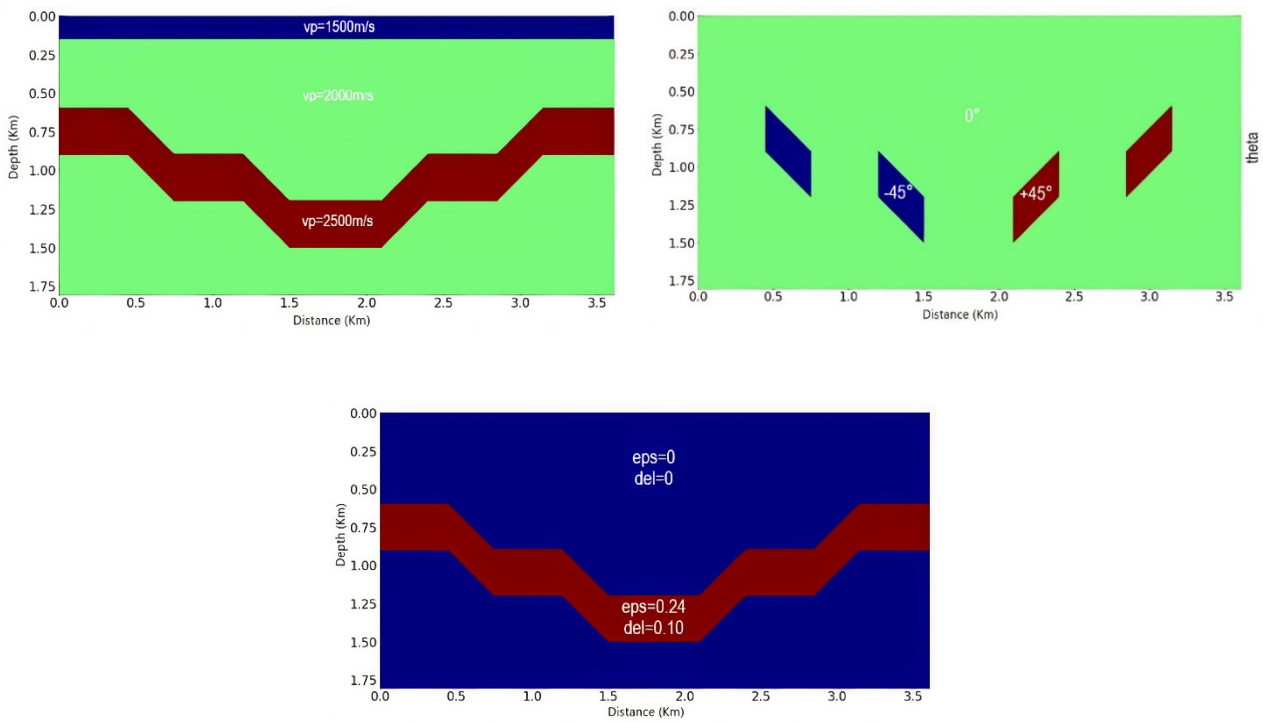


Figure 3 – Tilted model: P wave velocity (V_p), angle (θ), Thomsen parameters ϵ (0.24) and δ (0.1).

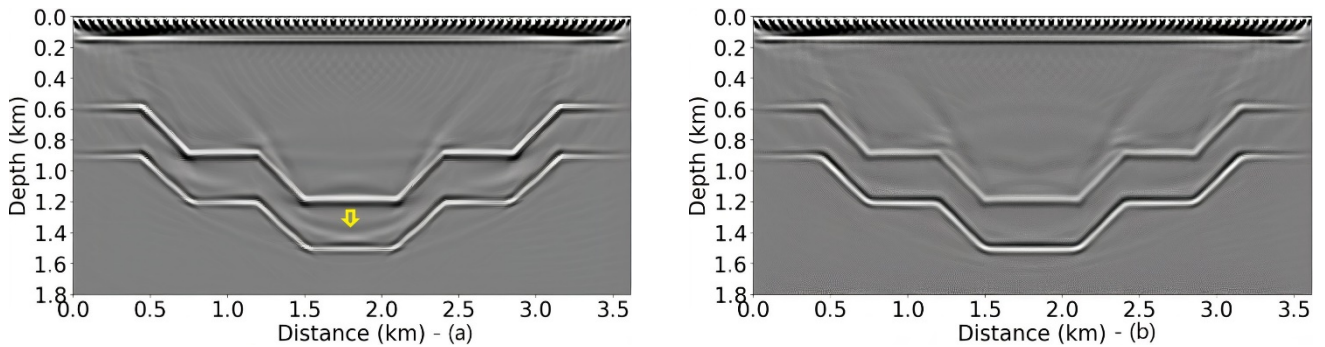


Figure 4 – Isotropic and TTI image in the case study I.

Case study II

This case study corresponds to the application of RTM in a model with anticline structure. Anticline layers are one of the components for a structural oil trap, in which it is caused by the tectonism of

the geological environment, or by the movement of salt in the subsurface; diapirism (Zou et al., 2015). In this context, a model was created simulating an oil reservoir containing only one anisotropic layer, whose inclination angles in the media are in opposite directions (Fig. 5).

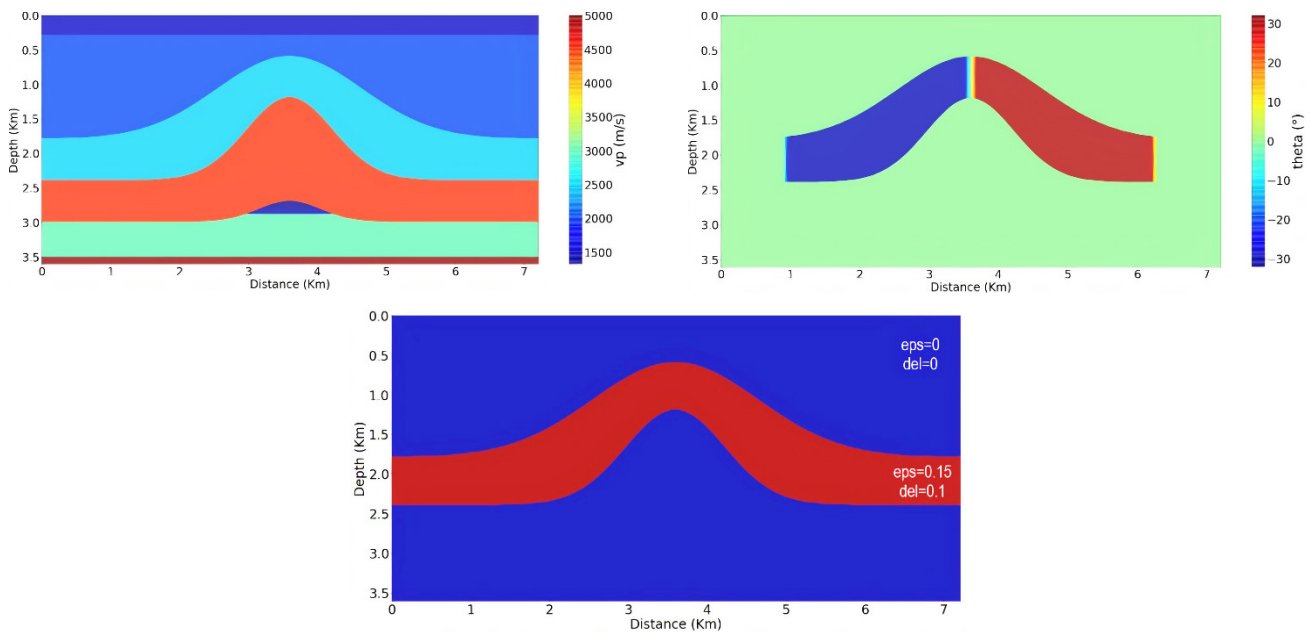


Figure 5 – Anticlinal model: P wave velocity (V_p), angle (θ), Thomsen parameters ϵ (eps) and δ (del).

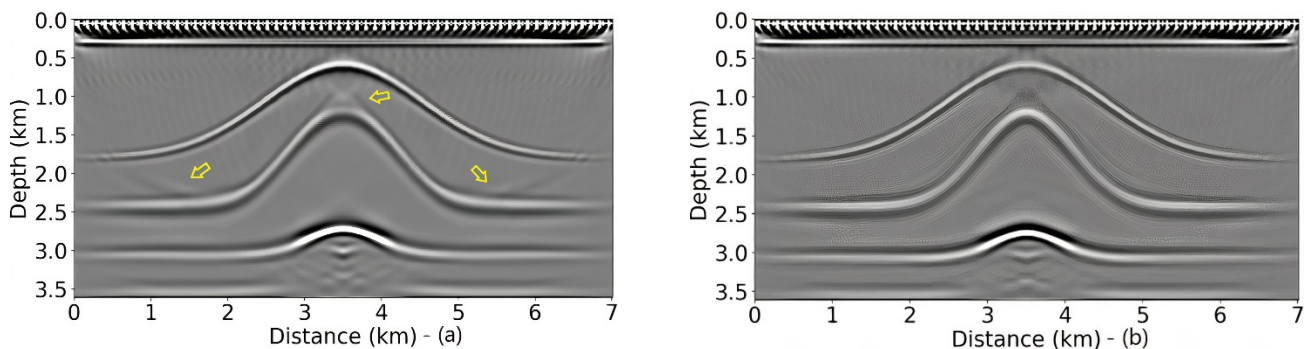


Figure 6 – Isotropic and TTI image in the case study II.

The model dimensions are 7,200 km in x-axis and 3,600 km in z-axis. Regarding the P wave velocity model, it initially contains a water depth of 1500 m/s, after the velocity increases 500 m/s in each layer, except for the salt body with 4500 m/s (in red). The basement has 5000 m/s, the oil 1325 m/s. Was included in this model one anisotropic layer, above the salt, where the values of ϵ , δ and are 0.15, 0.1, respectively, and the angles of symmetry are

+35° and -35°, as shown in Figure 5(b).

The synthetic shot data was generated by the Equation (2) and include 60 shots with distance between shots of 120 m. The grid space used was $h = 12$ m and a Ricker wavelet of 30 Hz cutoff frequency was applied. The acquisition geometry used was, similar to the first case study, a fixed spread where only the seismic source moves. The results for the acoustic isotropic RTM and TTI pseudo-acoustic RTM are shown at Figure 6.

In Figure 6 there are minor errors, specially some artefacts that are uncorrelated to the original model (pointed with yellow arrows). These errors are small because the small offsets and the reflectors are well imaged due to yet small offset and simplicity of the model. As soon as the model complexity and offset increase the isotropic RTM will not be able to correctly image the reflectors, as will be seen next.

Case study III

In the third case study, part of the BP TTI 2007 benchmark model was migrated. The synthetic data was generated by Hemang Shah through an elastic modeling by finite differences and it is available on the SEG website as a courtesy by BP Exploration Operation Company Limited. The BP TTI 2007 benchmark model is ideal to test TTI algorithms. It very complex and it has high similarity with a real data, thus it is widely used for the purpose of validation of migration algorithms in TTI media.

As mentioned, only a small part of the model was migrated: it varies from 25 km to 40.625 km on x-axis and 11.25625 km on z-axis. The benchmark shot data was generated with an end-on acquisition geometry, where the streamer length is equal to 10 km and the minimum and maximum offset are 37.25m and 10025m, respectively. The depth of the source is 6m and the receiver is 8m. The shots interval is 50m and in the whole model. The number of receivers are equal to 800 channels spaced in 12.5m. The registration time of the fields in the survey is 9,208 s sampled at a rate of 8 ms.

The parameters used in the finite difference to model wave propagation for isotropic and TTI RTM were $h = 6.25$ m and $\Delta t = 0.5$ ms, applying a Ricker wave let with a 45 Hz cutoff frequency.

A characteristic in this part of the model is the abrupt variation in the symmetry angle near to thinner canopy feeder of the salt body (Fig. 7) with a variation of approximately $+45^\circ$ and -45° . This type of characteristic is responsible for the instability in direct modeling, generating spurious events in the images that are unrelated to the model. Therefore, some actions were used as the smoothing of parameters ε , δ and θ and use of the sigma parameter equal to 0.7.

As the first two case studies, two migrations were performed, one for the acoustic case and another for the TTI case. Regarding the number of shots, 100 shots were chosen to proceed the migration. The migration results are shown in Figure 8. The TTI anisotropic RTM migration was capable of imaging the BP TTI 2007 benchmark model much better than the isotropic imaging algorithm.

CONCLUSION

This paper discussed the implementation of the reverse time migration for tilted transversely isotropic media applying pseudo-acoustic wave equation. The developed algorithm was applied to three case studies using synthetic models with growing complexity. The last one was a selected part of the BP TTI 2007, a very complex and realistic model used as benchmark.

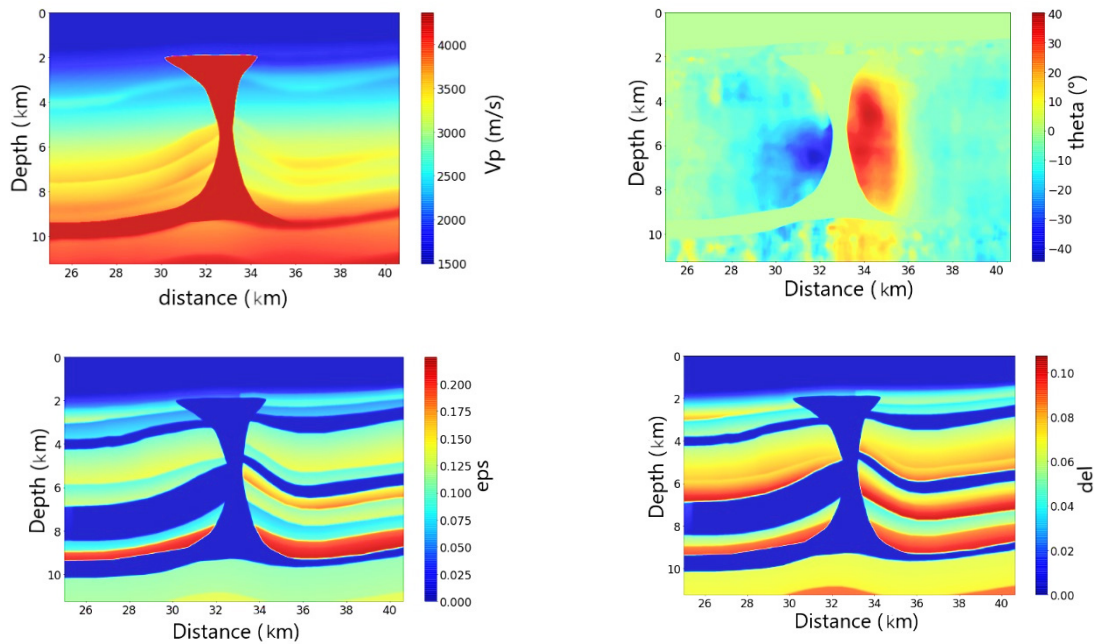


Figure 7 – BP TTI 2007 Model.

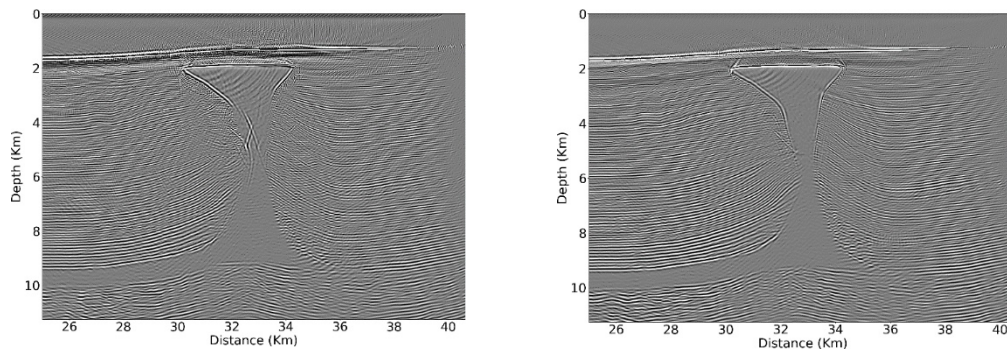


Figure 8 – Isotropic and TTI image in the case study III.

As expected, in all cases, the TTI algorithm presented better results than isotropic migration. However, only when the offset is large and complexity is big enough, the TTI RTM algorithm produces results significantly better. The last case study, where was used the BP TTI model, the maximum offset is 10 km and the thinner canopy feeder of the salt body has high tilt angles and angles of symmetry. In this case, the image of the salt structure and adjacent layers

using TTI RTM is much better focused.

REFERENCES

- ALKHALIFAH T. 2000. An acoustic wave equation for anisotropic media. *Geophysics*, 65(4): 1239–1250.
- BAYSAL E, KOSLOFF DD & SHERWOOD JWC. 1983. Reverse time migration. *Geophysics*, 48(11): 1514–1524.
- BOS L, GIBSON P, KOTCHETOV M & SLAWINSKI

- M. 2004. Classes of anisotropic media: a tutorial. *Studia Geophysica et Geodaetica*, 48(1): 1573–1626.
- CLAERBOUT JF. 1971. Toward a unified theory of reflector mapping. *Geophysics*, 36(3): 467–481.
- FLETCHER RP, DU X & FOWLER PJ. 2009. Reverse time migration in tilted transversely isotropic (TTI) media. *Geophysics*, 74(6): WCA179–WCA187.
- FOWLER PJ, DU X & FLETCHER RP. 2010. Coupled equations for reverse time migration in transversely isotropic media. *Geophysics*, 75(1): S11–S22.
- HELBIG K & THOMSEN L. 2005. 75-plus years of anisotropy in exploration and reservoir seismic: A historical review of concepts and methods. *Geophysics*, 70: 9ND–23ND.
- RAMÍREZ AC & WEGLEIN AB. 2009. Green's theorem as a comprehensive framework for data reconstruction, regularization, wavefield separation, seismic interferometry, and wavelet estimation: A tutorial. *Geophysics*, 74(6): W35–W62.
- RUDZKI MP. 1897. Über die Gestalt elastischer Wellen in Gesteinen. *Bulletin International de l'Académie des Sciences de Cracovie*, p. 387–393.
- RUDZKI MP. 1912. Sur la propagation d'une onde élastique superficielle dans un milieu transversalement isotrope. *Bulletin International de l'Académie des Sciences de Cracovie (IA)*, pp. 47–58.
- THOMSEN L. 1986. Weak elastic anisotropy. *Geophysics*, 51(10): 1954–1966.
- ZHOU H, ZHANG G & BLOOR R. 2006. An anisotropic acoustic wave equation for modeling and migration in 2D TTI media. In: 76th Annual Meeting. New Orleans, Louisiana: Society of Exploration Geophysicists. p. 194–198.
- ZHU T. 2014. Time-reverse modelling of acoustic wave propagation in attenuating media. *Geophysical Journal International*, 197(1): 483–494.
- ZOU C, ZHAI G, ZHANG G, WANG H, ZHANG G, LI J, WANG Z, WEN Z, MA F, LIANG Y, YANG Z, LI X & LIANG K. 2015. Formation, distribution, potential and prediction of global conventional and unconventional hydrocarbon resources. *Petroleum Exploration and Development*, 42(1): 14–28.

Recebido em 9 de março de 2020 / Aceito em 9 de setembro de 2020

Received on March 9, 2020 / Accepted on September 9, 2020